



An intelligent recommendation system for personalised parametric garment patterns by integrating designer's knowledge and 3D body measurements

Cheng Chi, Xianyi Zeng, Pascal Bruniaux & Guillaume Tartare

To cite this article: Cheng Chi, Xianyi Zeng, Pascal Bruniaux & Guillaume Tartare (28 Mar 2024): An intelligent recommendation system for personalised parametric garment patterns by integrating designer's knowledge and 3D body measurements, Ergonomics, DOI: [10.1080/00140139.2024.2332772](https://doi.org/10.1080/00140139.2024.2332772)

To link to this article: <https://doi.org/10.1080/00140139.2024.2332772>



Published online: 28 Mar 2024.



Submit your article to this journal 



Article views: 335



View related articles 



View Crossmark data 

RESEARCH ARTICLE



An intelligent recommendation system for personalised parametric garment patterns by integrating designer's knowledge and 3D body measurements

Cheng Chi^{a,b,c}, Xianyi Zeng^b, Pascal Braniaux^b and Guillaume Tartare^b

^aWuhan Textile University, Wuhan, China; ^bEcole Nationale Supérieure des Arts et Industries Textiles, GEMTEX Laboratory, Roubaix, France; ^cWuhan Textile and Apparel Digital Engineering Technology Research Center, Wuhan, Hubei, China

ABSTRACT

Garment pattern-making is one of the most important parts of the apparel industry. However, traditional pattern-making is an experience-based work, very time-consuming and ignores the body shape difference. This paper proposes a parametric design method for garment pattern based on body dimensions acquired from a body scanner and body features (body feature points and three segmented body part shape classification) identified by designers according to their professional knowledge. By using this method, we construct a men's shirt pattern recommendation system oriented to personalised fit. The system consists of two databases and three models. The two databases include a relational database (Database I) and a personalised basic pattern (PBP) database (Database II). The Database I is based on manual and three-dimensional (3D) measurements of human bodies by using designer's knowledge. And Database I is a relational database, which is organised in terms of the relational model of the body part shape and its key body feature dimensions. After a deep analysis of measured data, the irrelevant measured dimensions to human body shape have been excluded by designers and extract representative human body feature dimensions. In addition, the relations between body shapes and previously identified body feature dimensions have been modelled. From the above relational model, we label key feature point positions on the corresponding 3D body model obtained from 3D body scanning and correct the whole 3D human upper body model into the semantically interpretable one. The 3D personalised basic pattern is drawn on the corrected model based on these key feature points. By using three-dimensional to two-dimensional (3D-to-2D) flattening technology, a 2D flatten graph of the 3D personalised basic pattern of the interpretable model is obtained and slightly adjusted to the form suitable for industrial production, i.e., PBP and the PBP database (Database II) is built. In addition, the three models include a basic pattern parametric model (Model I) (characterizing the relations between the basic pattern and its key influencing human dimensions (chest girth and back length)), a regression model (Model II) which enables to infer from basic pattern to PBP for three body parts based on the one-to-one correspondence of key points between the PBPs and the basic patterns and a personalised shirt pattern parametric model (Model III) (characterizing the structural relations between the personalised shirt pattern (PBPshirt) and PBP). The initial input items of the recommendation system are the body dimension constraint parameters, including chest girth, back length and the body feature dimensions used to determine each body part shape as well as three shirt style constraint parameters (slim, regular and loose). By using Model I, the corresponding basic pattern can be generated through the user's chest girth and back length. Body feature dimensions determine the three body parts' shapes. Then, Model II is used to generate the PBP for the corresponding body parts shape. Based on the shirt style chosen by the user, Model III is used to generate the PBPshirt from the PBP. The output of the recommendation system is a fit-oriented PBPshirt. Moreover, if the PBPshirt is unsatisfactory after a virtual try-on, four adjustable parameters (front side-seam dart, back side-seam dart, waist dart and garment bodice length) are designed to adjust the PBPshirt generated by the proposed recommendation system.

Practitioner summary: The proposed recommendation system combines the designer's knowledge of manual measurement of the human body, traditional 2D pattern-making methods and 3D-to-2D flattening technology to generate personalised shirt patterns automatically and quickly, thus significantly improving pattern-making efficiency. The reliance on designers in the garment production process is reduced. Even users with no pattern-making knowledge can also develop professional shirt patterns by using our proposed system.

ARTICLE HISTORY

Received 13 June 2023
Accepted 3 February 2024

KEYWORDS

personalised pattern-making; designer's knowledge; fit oriented; parametric modelling, body parts segmentation

1. Introduction

Garment fit is one of the key elements of garment quality and customer satisfaction, which determines whether the produced garments can be chosen by more people (Song and Ashdown 2012). Due to the increase in consumption levels and changes in the diet of people, the body dimensions of different consumer groups are becoming more and more different, which has led to the fact that the anthropometric data on which ready-to-wear sizing system has been based is obsolete. The produced garments based on this system do not fit current body dimensions (Pierola, Epifanio, and Alemany 2016). Personalised customisation is considered to be an effective way of improving the fit of garments (Su, Liu, and Xu 2015; Su et al. 2017; Zhou, He, and Li 2017). However, with the popularity of personalised customisation, garment pattern-making as a key factor to improve the efficiency of garment production (Liu et al., 2016; Liu, Zeng, Wang, et al. 2018) needs to become faster and better.

Whether through traditional manual garment pattern-making or computer-aided design (CAD) software (Deivanayagam 1992), the pattern designers need to have a great wealth of professional knowledge and proficient skills to make a better-fit garment pattern quickly (Gu, Liu, and Xu 2017; Belhadi et al. 2019). Meanwhile, these methods also have the following disadvantages (Kang and Kim 2000; Liu, Wang, and Hong 2017): (1) the learning process is particularly long and difficult to promote and the making process is time-consuming, limiting the improvement of production efficiency. Although the CAD garment pattern-making software can automatically grade, which improves production efficiency, it is only suitable for the overall grading of the standard dimension specifications. It cannot automatically adjust the changes of individual dimensions; (2) once the garment style changes, the structure drawing of the garment needs to be manually redrawn or adjusted, which cannot automatically and quickly respond to the adjustment of the garment pattern.

To solve the above problems, researchers have developed some new techniques for generating garment patterns. The garment pattern generation technique based on an artificial neural network (ANN) simulates the designer's pattern-making process, defining the anthropometric dimensions as the input data of this model and the X, Y coordinates of the garment pattern as the output data of this model (Xiu and Wan 2013). Chan et al. proposed an ANN model to predict the pattern parameters of men's shirts (Chan, Fan, and

Yu 2003). Liu et al. developed a backpropagation artificial neural network (BP-ANN) model to predict the lower body dimensions used for pants pattern design (Liu, Wang, and Hong 2017). Wang et al. proposed a radial basis function artificial neural networks (RBF-ANN) predictive model to improve the prediction accuracy of body dimensions used for garment pattern-making (Wang, Zhang, et al. 2019). The key technique of these methods is to establish the relationship between the human body data and the garment pattern. However, the garment pattern is a combination of curves and straight lines, which is difficult to describe using specific data, resulting in unreasonable output garment patterns. Therefore, it is limited to simple garment patterns and is not widely used.

There are also many researchers who are exploring the method of creating garment patterns directly from 3D human body models, i.e., 3D-to-2D flattening technology (Thomasset and Bruniaux 2013; Hong et al. 2016). Hong et al. even used this technology to design personalised garments for physically disabled people with scoliosis. A pattern modification model that utilises the designer's expertise to evaluate the 3D virtual fitting results was proposed. The study results showed that 3D to 2D garment design can effectively realise the personalisation of atypical forms (Hong, Bruniaux, and Zhang 2018). However, the current 3D human body models applied in the apparel industry are mostly rigid, lack human body interpretation information, such as skeletal structure, body composition (bone, fat and muscle) and body deformation associated with skin elasticity and movement (Malhotra et al. 2019; Jeang et al. 2018; Malti 2021). For example, the most serious problem in 3D garment design and anthropometry is the lack of feature anthropometric point labels. Many anthropometric points on the bones, which are usually manually identified by designers, cannot be accurately determined from the 3D human model surface shape. It is impossible for most designers who lack the knowledge of anthropometry to respond quickly and effectively when using such 3D human body models to design. In addition, this method does not accurately determine the ease allowance between the body and the garment. Therefore, it is only suitable for designing simple and tight-fitting garments.

Compared with the methods mentioned above, the parametric garment pattern-making technology can better satisfy the requirements of the apparel industry (Liu, Zeng, Wang, et al. 2018). By defining the geometric and dimensional relationships between the various geometric objects in a garment pattern, a garment

pattern can be quickly adjusted by dimension-driven to generate the new garment pattern (Cui 2016; Leong, Fang, and Tsai 2007). In garment pattern-making, both body shape and dimension are significant for garment fit (Liu, Wang, and Hong 2017). Jin et al. proposed a new method for the automatic generation of personalised patterns. The method can estimate body size and design style by extracting contours from human body images. General pattern generation rules are established by analysing the basic rules between patterns and human body sizes and knowledge-based combinations of basic pattern and style parameters (Jin et al. 2023). However, most similar studies of parametric garment patternmaking techniques have considered only the differences between sizes. For this reason, the made garment patterns tend to ignore the individual shape differences, such as the convex chest, rounded back and slipped shoulders, which reduces the custom garment fit (Fengqin et al. 2017). Although researchers have proposed some methods of garment pattern adjustment to eliminate body part unfit, such as shoulder unfit, there is no systematic adjustment method to improve the overall garment fit (Kim et al. 2017; Huang 2014). Therefore, it is significant to propose a fit-oriented personalised parametric garment pattern-making method that considers both human body dimension differences and each body part shape differences to help consumers, especially those not in the standard body shape and dimension, achieve the rapid generation of personalised garment patterns.

The purpose of this study is to propose a recommendation system for personalised patterns by using a parametric garment pattern-making hybrid model integrating the designer's pattern-making knowledge and anthropometric knowledge and 3D-to-2D flattening technology. Suppose the user is not satisfied with the result. In that case, feedback can be given to adjust the garment pattern until the garment pattern fits the body well. The approach includes five operations, the details will be explained in detail in Chapter 2.

2. Overview of the modelling procedure

In this paper, we use five operations described previously for conducting parametric modelling of the PBPshirt pattern-making. Figure 1 shows an overview of the proposed modelling procedure, the steps of which are summarised as follows.

a. In this process, we first need to construct a database of the human body (Database I) based on manual and 3D measurement. Designer's knowledge of measurement and three manual measurement methods are used, including body surface measurements

(Martin's ruler and tape measurements), two-dimensional photogrammetry and gypsum paper film flattened graph measurements (Mashiko 2006; Dianat, Molenbroek, and Castellucci 2018). Compared with 3D measurements, manual measurements can label the body feature points according to the body's skeletal features, enabling the generation of an interpretable human model. In addition, using gypsum paper film flattened graph measurements can acquire data from hidden body areas that 3D body scanners cannot measure. This is important for improving the 3D human model towards a real human body shape. Second, before body shape classification, each male upper body is segmented into three parts (arm roots, shoulders and torso [below the shoulders]) based on the designer's knowledge manually. This classification enables the precise extraction of interpretable key features on human body shapes. The accurate human body parts classification can enhance well-fitted garments. Third, at data analysis level, after validation of the acquired data by using the Kaiser-Meyer-Olkin test and Bartlett test (Dziuban and Shirkey 1974), we apply principal factors extraction to reduce the dimensionality of the measured anthropometric data by projecting them onto a low-dimensional subspace, where each axis (factor) is a linear combination of the initial variables (items) (Hammond et al. 2004; Lei, You, and Abdel-Mottaleb 2016; Peres, Mehta, and Ritchey 2017; Fan et al. 2019). To provide a convenient measurement for users, we only find one feature dimension (representative) from each principle factor and then use these items for body classification. Finally, the K-means clustering method (Hinds, McCartney, and Woods 1991; Hamad, Thomassey, and Bruniaux 2017) is used to classify each body part. The number of classes is determined by using analysis of variance (ANOVA).

Based on the above feature dimensions, the 3D human body model obtained from the scan (whole-body range laser scan) can be labelled and corrected. Before the process of labelling the 3D human body model, the acquired 3D human body data need to be pre-processed by using the reverse engineering modelling software, permitting filtering and hole-filling of the 3D human body model. Second, by combining with the three-view of the human body obtained from the method of 2D photogrammetry, the feature point positions are converted into coordinate positions in the 3D space and then are mapped onto a pre-processed 3D human body model. This step will significantly help the designers design garments accurately and efficiently on the scanned 3D human body model. The labelled 3D human body model can also provide design references for the 3D human body

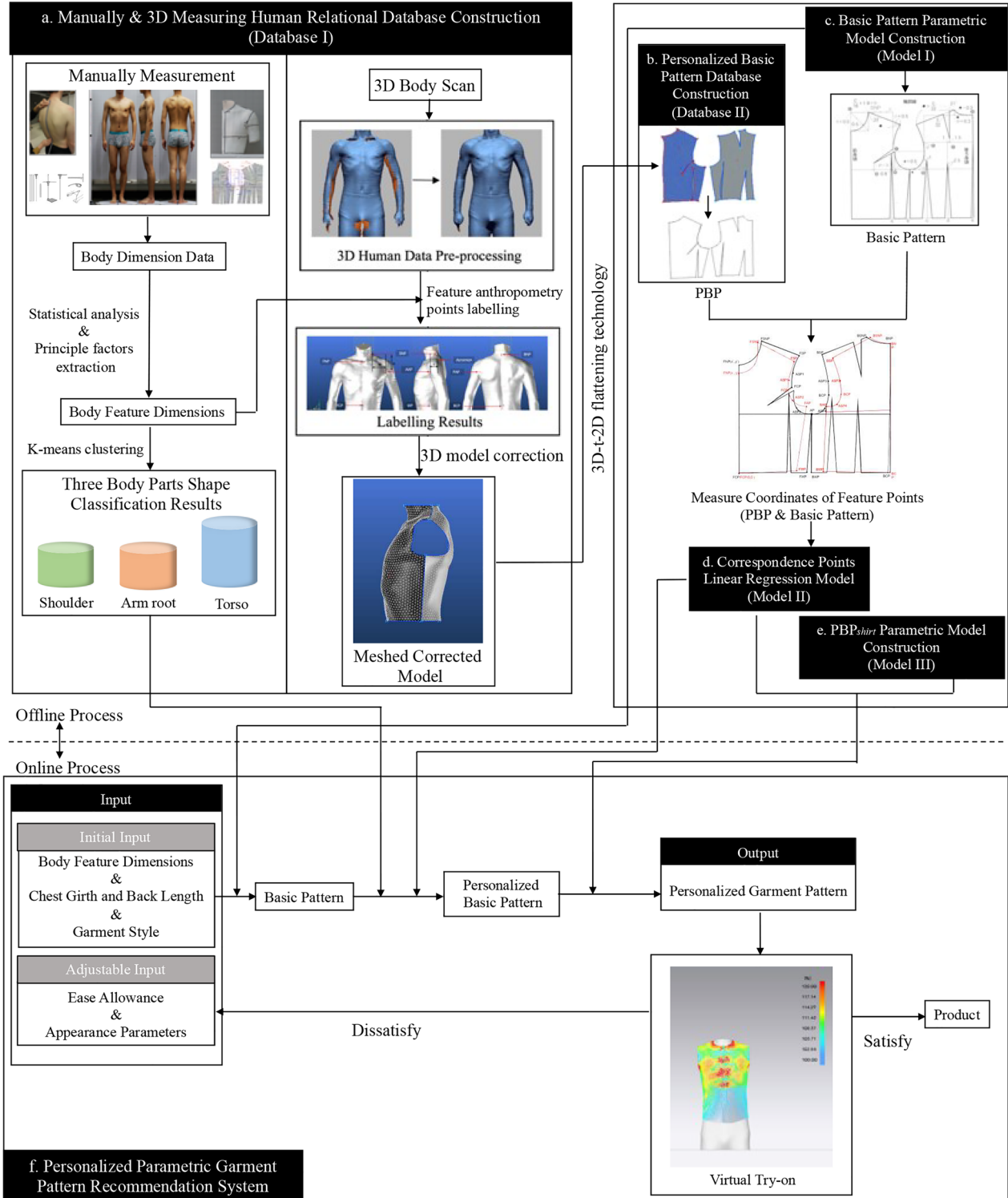


Figure 1. Overview of the proposed recommendation system.

model segmentation. There is no doubt that the human body structures (skeletons, muscles, etc.) can be considered in these labelled feature points on the revised 3D human model, which is initially a rigid geometric surface only. In addition, labelling the 3D

human body model can also correct the preprocessed models.

b. The 3D personalised basic pattern is drawn on the corrected model based on these key feature points. 2D flattened graphs of the 3D Basic Patterns are

obtained by using the 3D-to-2D flattening technology from the corrected 3D human body model. Based on the designer's knowledge, the 2D flattened graph of the 3D basic pattern is adjusted to a type suitable for industrial production, namely the PBP. Moreover, to construct the PBP database will be used to adjust the corresponding basic pattern.

c. In this process, we first build a parametric model of the basic pattern (Model I) (using the New Bunka basic pattern as an example) which characterises the relations between the basic pattern and its key influencing dimensions (chest girth and back length) (using the New Bunka prototype as an example). With this model, users only need to enter key dimensions to get their basic pattern. However, this basic pattern is based on a small number of body dimensions and fix algorithms, which ignores the differences among human body shapes and cannot be considered as a personalised basic pattern and needs to be adapted for personalisation.

d. To solve the above problem, a regression model (Model II) is established, which enables to infer from basic pattern to PBP for three body parts. First, the coordinates of each key structural point on the PBP and the basic pattern are measured separately. Then, the relation between each one-to-one corresponding point is built. In view of the influence of body shape differences on the garment pattern, every kind of body part shape corresponds to a linear relationship. Model II can predict the PBP from the basic pattern.e. A personalised parametric garment pattern model of different styles (Model III) (using male shirts as an example) is built. Model III can characterise the structural relations between the PBP_{shirt} and PBP. The principle is based on the prototype pattern-making method (Yumiko, et al. 2006).

f. The process of generating the PBP_{shirt} is automatic and rapid. The user only needs to enter the required body feature dimensions and select the style of the shirt. Through Database I, the recommendation system will automatically determine the user's body shape based on the dimensions entered by the user and determine the regression relationship (from basic pattern to PBP) corresponding to the body shape. Meanwhile, through Model I, a basic pattern of the user is automatically generated. Then, by using Model II and the regression relationship determined before, a PBP is automatically generated. Next, through Model III, a PBP_{shirt} is automatically generated for the style chosen by the user. By using virtual try-on technology, the garment pattern is assembled onto the corrected 3D human body model. Finally, the user evaluates the virtual garment. The garment is produced if the result

is satisfactory; otherwise, the pattern is adjusted by using adjustable parameters until it satisfies the requirements.

3. Extraction of initial input parameters

The initial input parameters of the proposed recommendation system in this study are divided into two groups: the initial input parameters of the basic pattern and the initial input parameters of the human body shape. The initial input parameters for the basic pattern are the key variables for making the pattern (i.e., chest girth and back length). And the initial input parameters of body shape are the body feature dimensions that are finally extracted after manual measurement and data analysis.

The manually anthropometric dataset used in this study is based on the measurements of 33 young males aged 18 to 25. The impacts of race, socioeconomic status and lifestyle were considered to some extent. They do not have morphological deformities (e.g., skeletal, joint and muscle deformities) and physical disabilities and represent the general young male population.

3.1. Manually human body data acquisition

For each subject, three manual measurement methods are used. The measurement items include length, width, height, perimeter and angle data (Mashiko 2006). We use the human skeletal structure as the basis for manual measurements, combined with designer's anthropometric knowledge (e.g., Table 1), to make manual measurements more accurate and interpretable. We label key feature points manually on the real human body, such as shoulder points, front neck points, etc. Finally, 42 manual measurements have been measured, as shown in Figure 2. Each measurement has to be repeated to minimise errors. The statistical values of anthropometric parameters for the subjects used in this study are presented in Table 1.

3.2. Segmentation of upper body shape and basic pattern

As shown in Figure 3(a), to ensure the accuracy and comprehensiveness of the body classification results, the upper body of the subject is manually segmented into three parts (arm root, shoulder and torso [below the shoulder]) according to the designers' knowledge and structural characteristics of the young male upper body (Chi et al. 2022).

Table 1. Measurement items for young males and anthropometric statistics used in this study.

No.	Measurement method	Body measurement	Body parts	Abbreviation	Mean	SD	Min	Max
1	Body surface	Height	Torso (below the shoulder)	H	172.75	4.98	165.00	187.00
2		Axillary point height		APH	127.46	5.20	119.30	142.60
3		Anterior axillary point height		AAPH	130.76	5.02	122.30	146.20
4		Posterior axillary point to waistline		PAPH	129.27	4.85	122.10	144.80
5		Shoulder point height		SPH	140.02	5.00	132.50	156.10
6		Chest girth		CG	87.09	6.02	75.00	104.00
7		Chest arc length		CAL	34.88	3.13	29.40	40.50
8		Waist girth		WG	72.65	5.46	62.00	83.50
9		Anterior axillary point width		AAPW	32.56	1.66	28.70	35.80
10		Posterior axillary point to waistline		PAPW	33.45	2.16	29.20	38.00
11		Back arc length		BAL	38.05	4.46	32.00	58.00
12		Shoulder width	Shoulder	SW	37.98	2.25	33.70	43.90
13		Total shoulder width		SW(T)	42.57	4.04	37.00	56.00
14		Shoulder length		SL	14.34	2.30	10.00	23.50
15	2D photogrammetry	Upper chest tilt angle	Torso (below the shoulder)	UCIA	28.07	4.92	20.00	37.50
16		Lower chest tilt angle		LCIA	3.12	6.10	-12.00	16.00
17		Tilt angle of upper body axis		UBAIA	5.87	2.34	1.00	10.00
18		Upper angle of scapula		USIA	27.23	6.81	12.00	40.00
19		Angle of inclination of lower scapula		LSIA	10.81	6.33	-18.00	20.00
21		Chest thickness		CT	21.72	1.66	18.50	24.70
22		Waist thickness		WT	19.53	1.83	16.00	24.30
23		Front shoulder angle	Shoulder	FSA	24.64	3.39	18.00	30.00
24	Gypsum paper film flatten graph	Distance from shoulder point to waistline (front)	Torso (below the shoulder)	SWD(F)	36.75	2.54	29.60	42.00
25		Distance from shoulder point to waistline (back)		SWD(B)	35.99	2.48	30.40	40.40
26		Distance between the concave part of rare armhole arc and waistline		RAWD	24.05	2.41	19.00	28.40
27		Distance between the concave part of front armhole arc and waistline		FAWD	27.61	3.47	18.60	34.00
28		Distance from side neck point to chest line (front)		SNCD(F)	22.01	2.56	14.70	25.90
29		Distance from side neck point to chest line (back)		SNCD(B)	25.02	2.45	20.60	31.00
30		Front shoulder length	Shoulder	SL(F)	13.34	1.57	9.50	16.00
31		Back shoulder length		SL(B)	16.36	2.17	12.20	22.90
32		Back shoulder angle (°)		RSS	24.42	5.06	12.00	32.50
33		Front shoulder angle (°)		FSS	22.45	5.17	11.00	32.00
34		Armhole arc length (back)	Arm root	AAL(B)	19.31	4.59	1.30	30.40
35		Armhole arc length (front)		AAL(F)	19.92	1.95	15.50	23.60
36		Armhole arc length (total)		AAL(T)	39.24	5.56	18.40	50.00
37		Arm root depth		ARD	15.90	1.48	12.40	18.90
38		Arm root width		ARW	10.26	1.61	6.60	12.90
39		Distance between the back-shoulder point to the chest line		SCD(B)	17.78	3.29	13.30	26.20
40		Distance between the front-shoulder point to the chest line		SCD(F)	18.53	2.35	11.90	23.10
41		Distance between the most concave part of the rear-armhole arc to the chest line		RACD	5.84	3.00	1.00	12.50
42		Distance between the most concave part of the front-armhole arc to the chest line		FACD	9.40	3.40	3.60	17.60

Note: Mean stands for average; SD stands for standard deviation; Min stands for minimum; Max stands for maximum; Red font unit: °; Black font unit: cm.

To make the final obtained personalised basic pattern which is oriented to fit, the feature differences of body parts should be considered. The basic pattern is also considered as a combination of three parts in this study based on upper body shape segmentation results.

The basic pattern is made of points, straight lines and curves. Therefore, in this study, the segmentation of the basic pattern should consider the key feature points contained in each part and the coordinate position of the key feature points, as shown in Figure 3 (b).

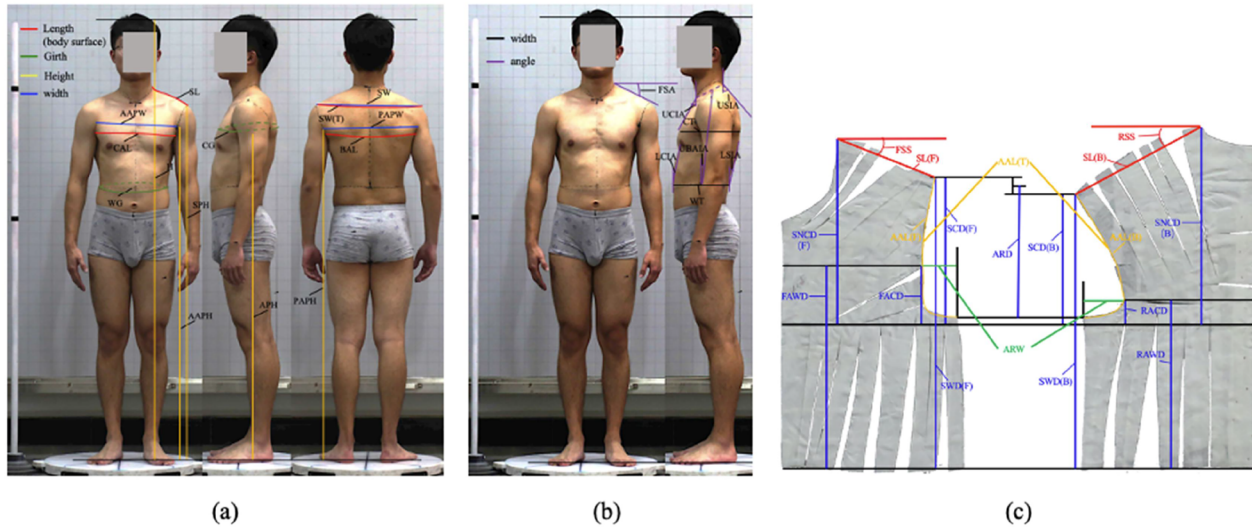


Figure 2. Manual measurement methods: (a) body surface measurement; (b) 2D photogrammetry measurement; (c) gypsum paper film flattened graph measurement.

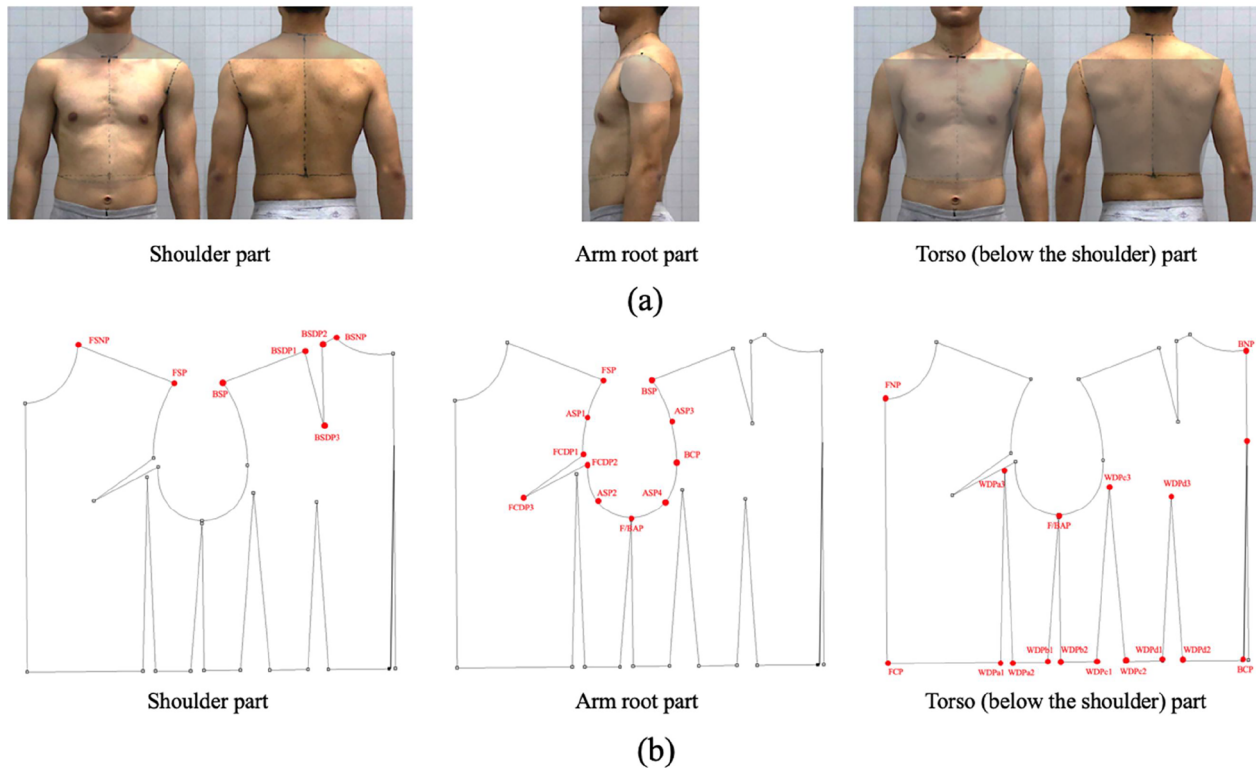


Figure 3. Upper body and basic pattern segmentation manually realised by designers.

3.3. Initial input parameter extraction for human body shapes

Factor analysis is a technique used to reduce a large number of variables into fewer numbers of factors (Yong and Pearce 2013). In this study, factor analysis aims to reduce the number of anthropometric dimensions and detect the structure in the relationships among anthropometric dimensions.

3.3.1. Kaiser–Meyer–Olkin test and bartlett test of sphericity

In this section, the Kaiser–Meyer–Olkin (KMO) test and Bartlett's test of sphericity are used to verify if the data distribution is relevant to factor analysis. The KMO value close to 1 generally indicates that the correlation between variables is strong. If the p-value from Bartlett's test of sphericity is lower than the

Table 2. KMO and Bartlett test.

KMO and Bartlett's Test					
Arm root	Kaiser–Meyer–Olkin Measure of Sampling Adequacy.			0.617	
	Bartlett's Test of Sphericity			Approx. Chi-Square	214.752
	df		df	36	
Shoulder	Kaiser–Meyer–Olkin Measure of Sampling Adequacy.			Sig.	0.000
	Bartlett's Test of Sphericity			Approx. Chi-Square	0.723
	df		df	28	
Torso (Below the shoulder)	Kaiser–Meyer–Olkin Measure of Sampling Adequacy.			Sig.	0.000
	Bartlett's Test of Sphericity			Approx. Chi-Square	0.568
	df		df	742.90	
			Sig.	231	
			Sig.	0.000	

Note: df stands for degrees of freedom; Sig. stands for minimum significance.

significance level, then our dataset is suitable for a data reduction technique. As shown in **Table 2**, all the test values of KMO are > 0.5 , and all significance (sig) values are 0. The original variables are considered to be correlated with each other and suitable for applying factor analysis (Zakaria 2014; Huang et al. 2021).

The parameter equations of KMO test (1) and Bartlett test (2) are as follow:

$$KMO = \frac{\sum \sum_{i \neq j} r_{ij}^2}{\sum \sum_{i \neq j} r_{ij}^2 + \sum \sum_{i \neq j, k} r_{ijk}^2} \quad (1)$$

$$X^2 = \frac{(N-k)\ln(S_p^2) - \left(\sum_{i=1}^k (n_i - 1)\ln(S_i^2)\right)}{1 + \frac{1}{3(k-1)} \left(\sum_{i=1}^k \left(\frac{1}{n_i - 1} \right) - \frac{1}{N-k} \right)} \quad (2)$$

3.3.2. Principal factors extraction

Considering the shoulder as an example, **Table 3** shows that the cumulative contribution of the first third factors is 87.3%. In our study, if the cumulative contribution rate threshold is 85%, we need to select the first third components. Therefore, we consider that all datasets can be represented by these third factors.

The maximum variance method is used to implement an orthogonal rotation of the factor loading matrix to clarify the meaning of the factors. The rotated factor loading matrix is shown in **Table 3**. The first principal factor has larger loadings on SW, SL, SW(T) and RSS, which is a composite reflection of the width of the shoulder; the second principal factor has larger loadings on SL(F), SL(B) and FSS, which is a composite reflection of the length of the shoulder; the third principal factor has larger loadings on FSA, which is a composite reflection of the angle of the shoulder. According to the meanings of the factors, factors 1, 2 and 3 are named width, length and angle factors, respectively. To make the user's measurement easy, a representative feature dimension from each principal factor is found. Then these items are used for body classification. The selection is based on a high

Table 3. Rotated component matrix of shoulder anthropometric measurement.

Body part	No.	Items	Rotated component matrix ^a		
			1	2	3
Shoulder	1	SW	0.898	0.157	0.031
	2	SL	0.857	0.037	0.168
	3	SW(T)	0.831	0.357	-0.035
	4	RSS	0.412	0.022	-0.050
	5	SL(F)	0.299	0.866	-0.005
	6	SL(B)	0.548	0.747	-0.091
	7	FSS	-0.378	0.723	0.388
	8	FSA	0.079	0.056	0.970
% of Variance			43.354	25.741	18.183
Cumulative %			43.354	69.095	87.278

Extraction Method: Principal Component Analysis. Rotation Method: Varimax with Kaiser Normalisation.

correlation with the corresponding principal factor and relative ease of measurement. Accordingly, representative feature dimensions for the shoulder include SW, SL(F) and FSA.

The arm root and torso (below the shoulder) are obtained representative feature dimensions for body classification by the same methods. The arm root feature dimensions include AAL(F), AAL(B), SCD(B) and ARW. The torso (below the shoulder) feature dimensions include PAPH, WG, SWD(B), CAL, UBAIA, BAL and LCIA.

3.4. Body part shape clustering

Based on the representative feature dimensions obtained previously, the K-means method was used to body part shape clustering. However, the K-means algorithm requires that the number of levels is determined before running. **Table 4** shows the ANOVA results when the third representative shoulder dimensions are clustered into categories three, four and five. When the experimental samples are divided into third and five levels, the probability of the F test is < 0.05 , showing that clustering into three and five classes is reasonable. For convenience of industrial production, we decide to divide the shoulder shapes into three classes.

As mentioned above, the K-means method is used to cluster the arm root shapes and torso (below the shoulder) shapes. The best results can be obtained when selecting four classes of arm root shapes and eight classes of torso (below the shoulder) shapes. Representative feature dimensions and classification results for the three body parts will be used to manually label and correct the scanned 3D human body models.

4. 3D Human body model correction

The 3D scanning instrument used is the OKIO-Body Scan 3D body scanning system (Beijing TEN YOUN 3D Technology CO. LTD). The scan is performed with both arms spread out at approximately 30°, the eyes looking forward and both feet in a fixed position. Multiple scans are obtained with the best choice based on the results.

4.1 3D Human data pre-processing

The 3D scan data are generally noisy and exhibit defects owing to the inaccessibility of hidden areas. A large hidden area, such as in the crotch and armpit, can result in large holes. Various data pre-processing operations, such as filtering and hole filling, are performed before reconstructing the model. The reverse engineering modelling software Geomagic Design X is

used to generate CAD models from the scanned data of the subjects.

4.2. Feature points labelling

The number and position of feature points can optimise the descriptive and discriminatory capabilities of the human model, which has been demonstrated in previous research (Chi et al. 2022). The following are the details of the operation: to correct the scanned 3D human body model, we determined ten human feature anthropometric points based on human skeletal features, extracted feature dimensions, anthropometric definitions and designer's knowledge, as shown in Table 5. These points are enough to extract the key morphological contour of the male upper body. We label six key feature points manually, including the lateral neck root point, the waist point, the front neck points, the cervical, the front central point and the back central point, as shown in Figure 4, on the real human body with black marker stickers before scanning. This is to realise quick and accurate findings of these points on the scanned 3D human body model. Then, the positions of the other four feature anthropometric points are measured and calculated using a three-view photograph of the human body (see in

Table 4. Analysis of variance in typical indices.

Parts	NO.	Items	Cluster		Error		F	Sig.
			Mean Square	df	Mean Square	df		
Shoulder	3	SW	34.389	2	3.259	30	10.551	0.000
		SL(F)	9.100	2	2.120	30	4.293	0.023
		FSA	139.108	2	3.336	30	41.699	0.000
	4	SW	32.530	3	2.378	29	13.679	0.000
		SL(F)	4.346	3	2.371	29	1.833	0.163
		FSA	94.132	3	3.307	29	28.466	0.000
	5	SW	29.926	4	1.673	28	17.885	0.000
		SL(F)	9.670	4	1.540	28	6.280	0.001
		FSA	64.728	4	4.264	28	15.181	0.000

Note: df stands for degree of freedom; F stands for F-statistics; Sig. stands for minimum significance.

Table 5. List of anthropometric key feature points used in this study.

NO.	Body feature point	Abbreviation	Definition
1	Front neck point	FNP	The intersection of the line connecting the superior border of the right and left lateral clavicular terminal with the median sagittal plane.
2	Front central point	FCP	The intersection point of the waistline with the front central line.
3	Lateral neck root point	SNP	At the lateral cervical triangle, the intersection of the anterior border of the trapezius muscle and the curve connecting the cervical fossa to the cervical point on the lateral part of the neck.
4	Waist point	WP	The maximum point of lumbar concavity on the left side of the body.
5	Cervical	BNP	The point of the tip of the seventh cervical spine.
6	Back central point	BCP	The intersection point of the waistline with the back central line.
7	Anterior axillary point	AAP	The point superior to the anterior axillary fissure.
8	Acromion		The most lateral point of the outer edge of the scapula, usually equal to the shoulder height.
9	Posterior axillary point	PAP	The point at the upper end of the posterior axillary fissure.
10	Armpit point	AP	The point at the lower edge of the axillary fissure, with a wooden stick inserted to identify this point.

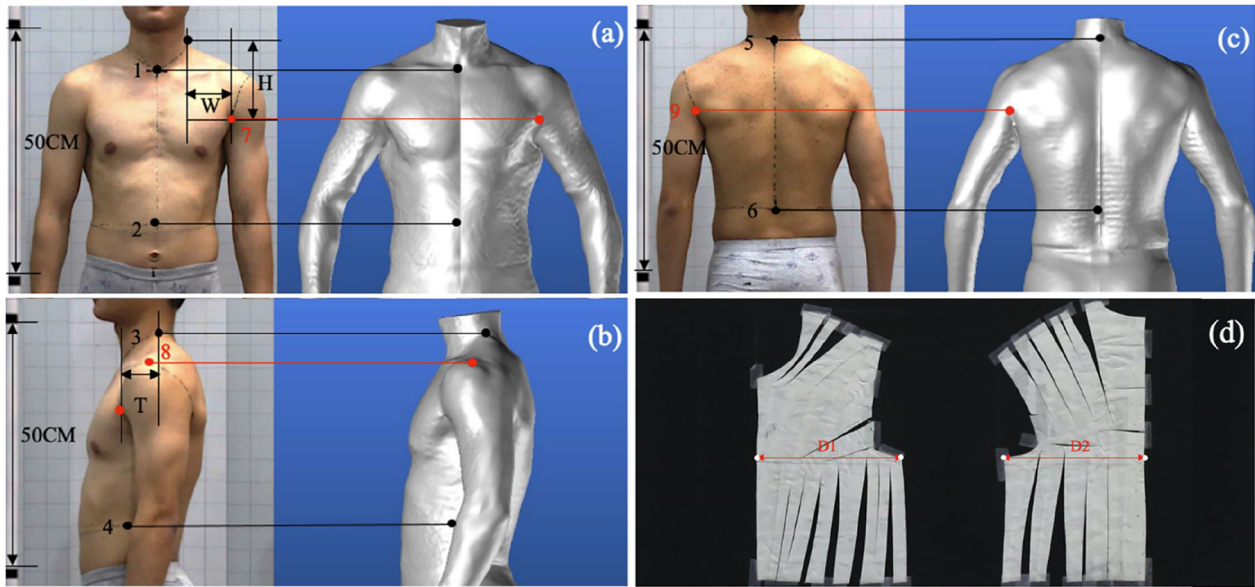


Figure 4. 10 key feature points correspondence for human body: (a) front view; (b) left side view; (c) back view; (d) Gypsum inner wall flatten graph (The white dots denote the intersection of the horizontal line of the armpit with the front centre line and the back centre line, respectively). Both red and black dots (marked before the 3D scanning) denote the feature points used in our experiments.

Figure 4(a–c)) obtained by two-dimensional photogrammetry. The method is to take the width difference (W), height difference (H) and thickness difference (T) among the measured points, as the coordinate values of the 3D coordinate system and establish a 3D coordinate system with a point as the origin. The positional relationship between other points and the origin is mapped to the 3D human model. In this study, the process is repeated twice with the lateral neck root point and the waist point as the coordinate origin, respectively, to reduce the errors generated in the mapping process. The final coordinate values of the other four feature anthropometric points are obtained as an average. In addition, the armpit point is different from other feature points because it is relatively hidden. The armpit point position cannot be determined directly from the three-view photos. For this reason, we need to measure the distances $D1$ and $D2$ from the armpit point to the front-back centreline (excluding the dart volume) with the help of the human body paper film flattening graph, as shown in Figure 4(d). The position of the armpit point has been calculated by combining the cross-section of the horizontal armpit line on the 3D model with the values of $D1$ and $D2$. It should be noted that the position is only an approximate position and is not necessarily accurate and needs to be adjusted later. This will be described later in this section.

4.3. Generation of the surface model

Based on the key feature items and key feature points, feature curves are drawn on the 3D human surface, as shown in Figure 5(a). The drawing method follows the anthropometric definition, as shown in Table 6. The drawing of the arm root curve is unique and significance, and the finished arm root curve (black curve, see in Figure 5(b)) is still different from the real arm root curve of the human body. To obtain a more accurate arm root curve, the parameter values need to be set in advance. The parameter values are represented by equal lines perpendicular to the black curve. The parameter curves (blue curve) were obtained by joining the other ends of all lines, as shown in Figure 5(b). The purpose is to change the shape of the arm root curve by adjusting the parameters to obtain the most similar arm root curve to the real human body. This method is original. It is significant for repairing the shape of the arm root. In addition, to build a model closer to the real human body, some human feature lines need to be drawn on the surface of the model, as shown in Figure 5(c). Figure 5(d) shows the surface model generated from the feature curves.

4.4. Generation of 3D-to-2D flattened graph

Meshing the new surface model, as shown in Figure 5(e). The model is processed by using the 3D-to-2D

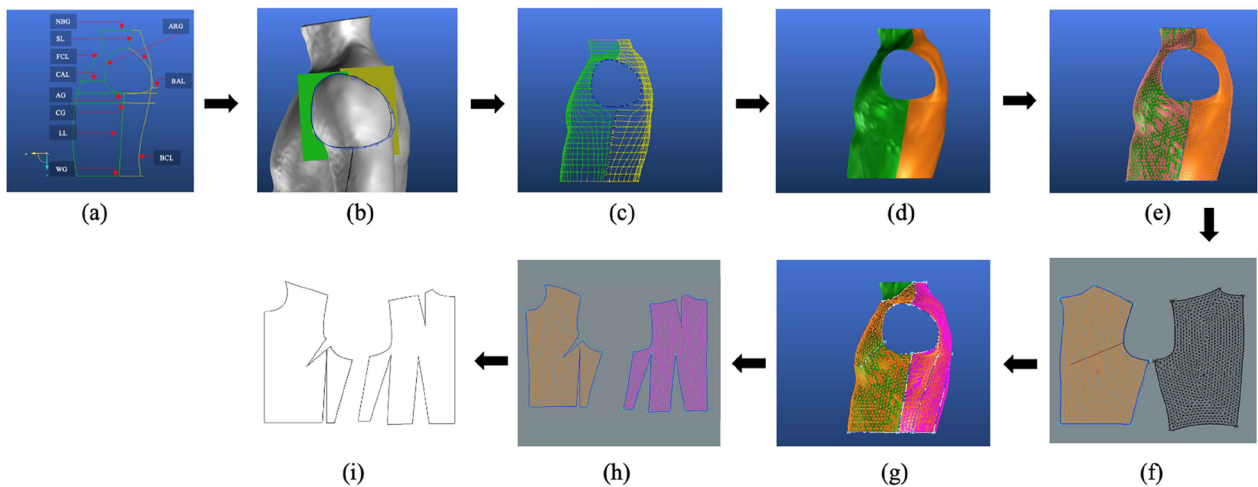


Figure 5. The PBP making process: (a) Drawing the human body features curve; (b) Drawing the arm root curve; (c) Adding body surface curves; (d) Generating human surface model; (e) Meshing human surface model. (f) A comparison of the 2D morphology of the 3D model with the flattened graph of the human paper film; (g) Drawing the basic pattern structure lines; (h) Generating 2D flattened graph of basic pattern; (i) Making the PBP.

Table 6. Upper body feature curves.

NO.	Body feature line	Abbreviation	Definition
1	Neck base girth	NBG	The horizontal circumference length through the lateral neck root point.
2	Shoulder line	SL	Measure the straight line distance from the lateral neck root point to the shoulder crest point.
3	Upper chest girth	AG	The horizontal circumference length through the posterior point of the left and right axilla.
4	Chest girth	CG	The horizontal circumference measured through the scapula, axilla and nipple.
5	Minimum waist girth	WG	The horizontal circumference of the smallest part of the waist between the inferior border of the ribs and the superior border of the iliac crest.
6	Front centre line	FCL	The length of the curve from the anterior neck point to the minimum waist circumference on the anterior centreline of the torso.
7	Back centre Line	BCL	The length of the curve from the posterior cervical point to the minimum waist circumference on the posterior centreline of the torso.
8	Lateral line	LL	Solid length from the waist point to the armpit point.
9	Chest arc line	CAL	Solid length of body surface from right anterior axillary point to left anterior axillary point.
10	Back arc line	BAL	Solid length of body surface from right posterior axillary point to left posterior axillary point.
11	Arm root girth	ARG	The length of the round curve through the acromion point, shoulder point, axillary anterior point and axillary posterior point.

flattening technology to generate the 2D flattened graph of this model. The arm root curve of the flattened graph is compared with the arm root curve (dark red curve) part of the human paper film flattened graph. In general, there are more or less differences between the two arm root curves. This is also mentioned in the previous section. The arm root parameters must be adjusted to get the most similar arm root curve to the real human body. The final result is shown in Figure 5(f). The overlapped results of the 2D flattened graph and the real arm root curve show the quality of morphological similarity given by the method. While adjusting the 2D flattened graph, the 3D shape of the model is also corrected. Then, drawing the basic pattern structure line on the corrected 3D model, as shown in Figure 5(g). Furthermore, it

must introduce some darts to generate the 2D flattened graph (Kim and Park 2007). Using the 3D-to-2D flattening technology again generates the 2D flattened graph of the basic pattern, as shown in Figure 5(h). Finally, the 2D flattened graph is slightly modified to meet the requirements for industrial production, i.e., PBP, as shown in Figure 5(i). The PBP obtained by this method will be used for overlapping comparison with the New Bunka basic pattern for the corresponding subject.

5. The parametric pattern-making method of PBPshirt

To research the method of personalised parametric garment pattern-making for different styles on the

PBP, this paper takes the personalised parametric pattern-making for the men's shirts body as an example, focusing on the calculation model, plotting method and programming of the front and back piece pattern structure of the basic pattern and PBPshirt, as well as the regression model from basic pattern to PBP.

5.1. The calculation model of the basic pattern

In the structural making of the New Bunka Men's upper body basic pattern (Yumiko et al. 2006), the key variables include chest girth and back length, as shown in Figure 6. After the calculation based on these key variables and the structural relationships inherent in the garment pattern, the values of the other secondary parameters are determined. Table 7 shows the expressions of the secondary parameters based on the key parameters. Regarding the darts, the New Bunka Men's upper body basic pattern contains the front chest dart, the back scapular dart and the waist darts (a, b, c, d, e), as shown in Figure 6. The front chest dart and back scapular dart can be obtained by using the formulas in Table 7. The volumes of waist darts are assigned as shown in Figure 6.

After being drawn, the intersections of the front and back centre lines with the waistline are used as the coordinate original points respectively (P_1 and P_2) in the New Bunka Men's upper body basic pattern in Figure 6). The relative coordinates of each key point of the front and back pieces are calculated. The

coordinates of the key points of the New Bunka Men's upper body basic pattern are shown in Table 8.

5.2. Adjusting the basic pattern

From the geometric perspective, a garment pattern can be considered as a set of geometric elements, including points, lines and curves (He et al. 2021). In this study, the points are considered as the basic elements to construct a basic pattern. By connecting the points, the outline of the basic pattern can be obtained. Therefore, the first step to adjust the basic pattern is to adjust the coordinate position of the key points that build the basic pattern. The 2D coordinate systems for the front and back pieces have been established separately by using the FCP and BCP as the origin, as shown in Figure 10. The coordinates of the corresponding points on the basic pattern and the PBP are measured separately. According to the position of the coordinate points, a linear regression model of the key points on the PBP and the corresponding key points on the basic model are developed. As is mentioned in 3.2, the basic pattern is also segmented like the upper body. Since there is a one-to-one relationship between the body shape and the basic pattern, body part shape differences are considered when the linear regression model is built.

Taking the shoulder as an example, the key points on the front shoulder are FSNP and FSP, and the points on the back shoulder are BSP, BSDP1, BSDP2, BSDP3

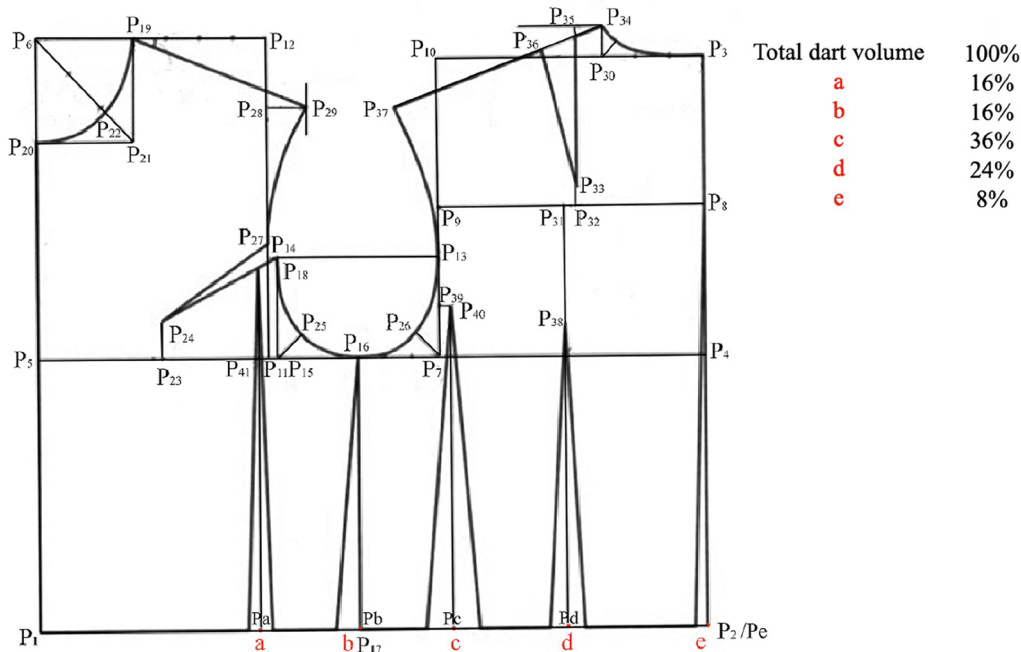


Figure 6. Structure of New Bunka men's basic pattern.

and BSNP, as shown in Figure 7. The coordinates of these seven key points are measured on the PBP and the basic pattern, respectively. The linear regression models are built based on the shoulder shape classification results and the coordinate values, as shown in Figure 8. According to the regression models, the coordinates of the points on the PBP can be predicted from the coordinates of the points on the basic pattern.

5.3. Plotting method

After obtaining the final coordinates of each key point, the matplotlib package of Python is used to draw straight lines on the basic pattern (Wang, Zhang, et al. 2019; Greder, Pei, and Shin 2020; Wang 2020). Drawing curves on the PBP outline is relatively complicated. In this paper, the Bézier curve model (Gu and Liu 2013;

Table 7. Structural relationship between dimensions of New Bunka men's basic pattern.

	No.	Line	Dimensioning formula		No.	Line	Dimensioning formula
Basic Lines	1	P1P2, P4P5	C/2+6,7	Contour Lines	20	P15P25, P7P26	1/6* (C/6-2,7)+0,5
	2	P2P3	B+0,5		21	P3P30	C/16+2,2
	3	P3P4, P7P10	C/6+8,5		22	P9P31	1/2* (C/6+5,8)+0,5
	4	P1P5, P2P4, P16P17	B-(C/6+8)		23	P31P32	1
	5	P4P7, P8P9, P3P10	C/6+5,8		24	P32P33	1.5
	6	P3P8, P9P10, P4P8, P7P9	(C/6+8,5)/2		25	P30P34	1/3* (C/16+2,2)-0,3
	7	P5P6, P11P12	C/4+2,5		26	P35P36	C/32
	8	P5P11, P6P12	C/6+2,9		27	P19P29	cos22°*(5/4*(5C/48+1)+1/2)
	9	P11P15, P14P18	0,7		28	P34P37	cos22°*(5/4*(5C/48+1)+1/2)+C/32
	10	P7P15, P13P18	C/6-2,7		29	P12P28	tan22°*(5/4*(5C/48+1)+1/2)
	11	P7P13, P15P18, P11P14	(C/6+8,5)/3		30	P31P38	(C/6+8,5)/2+-2,5
Contour Lines	12	P6P19, P20P21	C/16+1,9		31	P7P39	(C/6+8,5)/6
	13	P6P20, P19P21	C/16+2,4		32	P39P40	1
	14	P6P22	2/3* √(C/16+1,9) ² +(C/16+2,4) ² +0,5	Angle	33	P11P41	0,8
	15	P12P19	5C/48+1		34	∠P25P15P16	45°
	16	P28P29	1/4*(5C/48+1)+0,5		35	∠P39P7P16	45°
	17	P5P23	1/2* (C/6+2,9)+0,7		36	∠P12P19P29	22°
	18	P23P24	(C/6+8,5)/6-1		37	∠P42P34P37	21°
	19	P24P27, P18P24	P14P24=P18P24				

Note: C stands for chest girth and B stands for back length. All units are in cm.

Table 8. Coordinates of the key points of New Bunka men's basic pattern.

Point	Coordinate		Point	Coordinate	
	X	Y		X	Y
P1	0	0	P22	C/16+1,9-(5C+76)/40 *(1/3-1/2*√(C/16+1,9) ² +(C/16+2,4) ²	B+C/48-7,4+(5C+192)/80 *(1/3-1/2*√(C/16+1,9) ² +(C/16+2,4) ²
P2	C/2+6,7	0	P23	C/12+2,15	B-(C/6+8)
P3	C/2+6,7	B+0,5	P24	C/12+2,15	B-5C/36-91/12
P4	C/2+6,7	B-(C/6+8)	P25	C/6+3,6+cos45°*(1/6* (C/6-2,7)+0,5)	B-(C/6+8)+sin45°*(1/6* (C/6-2,7)+0,5)
P5	0	B-(C/6+8)	P26	C/3+0,9-cos45°*(1/6* (C/6-2,7)+0,5)	B-(C/6+8)+sin45°*(1/6* (C/6-2,7)+0,5)
P6	0	B+C/12-5	P27	C/6+2,9	√(C/12+1,45) ² +(C/36+29/12) ² -(C/12+3/4) ² -B-5C/36-91/12
P7	C/3+0,9	B-(C/6+8)			
P8	C/2+6,7	B-C/12-3,75	P28	C/6+2,9	B+C/12-5-tan22°*(5/4*(5C/48+1)+1/2)
P9	C/3+0,9	B-C/12-3,75	P29	37C/192+3,65	B+C/12-5-tan22°*(5/4*(5C/48+1)+1/2)
P10	C/3+0,9	B+0,5	P30	7C/16+4,5	B+0,5
P11	C/6+2,9	B-(C/6+8)	P31	5C/12+3,3	B-C/12-3,75
P12	C/6+2,9	B+C/12-5	P32	5C/12+4,3	B-C/12-3,75
P13	C/3+0,9	B-C/9-62/12	P33	5C/12+4,3	B-C/12-2,25
P14	C/6+2,9	B-C/9-62/12	P34	7C/16+4,5	B+C/48+28/30
P15	C/6+3,6	B-(C/6+8)	P35	5C/12+4,3	C/48+13/30-tan21°*(C/48+1/5)
P16	C/4+2,25	B-(C/6+8)	P36	5C/12+4,3-cos21°*C/32	C/48+13/30-tan21°*(C/48+1/5)-sin21°*C/32
P17	C/4+2,25	0	P37	7C/16+4,5-cos21°*(cos22°*(5/4*(5C/48+1)+1/2)+C/32)	B+C/48+28/30-sin21°*(cos22°* (5/4*(5C/48+1)+1/2)+C/32)
P18	C/6+3,6	B-C/9-62/12	P38	5C/12+3,3	B-C/6+10,5
P19	C/16+1,9	B+C/12-5	P39	C/3+0,9	B-5C/36-79/12
P20	0	B+C/48-7,4	P40	C/3+1,9	B-5C/36-79/12
P21	C/16+1,9	B+C/48-7,4	P41	C/6+2,1	B-(C/6+8)

Note: C stands for chest girth and B stands for back length.

Gu and Shi 2019; Liu et al. 2020) is used to accurately draw the cuff curves (FSP-ASP1-FCDP1, FCDP2-ASP2-FAP, BSP-ASP3-BCP-ASP4-BAP), the front collar girth curve (FSNP-ASP5-FNP) and the back collar girth curve (BSNP-ASP6-BNP) (see Figure 10). The Bézier curve model is:

$$B(t) = \sum_{i=0}^n \binom{n}{i} (1-t)^{n-i} t^i = \binom{n}{0} P_0 (1-t)^n t^0 \binom{n}{1} + P_1 (1-t)^{n-1} t^1 + \dots + \binom{n}{n-1} P_{n-1} (1-t)^1 t^{n-1} + \binom{n}{n} P_n (1-t)^0 t^n, \quad t \in [0, 1]$$

Where

Pi is the control point on the Bézier curve, P0 is the starting point, Pn is the end point and n is the order label of the points, starting from 0 and i is the order of the points, indicating the i-th point in the label, from 0 to n; t represents the time and takes the value of [0, 1], representing the change from 0 to 1.

The function Bézier curve (x , y) is written in Python based on the general formula of the Bézier curve. The input x is an array of horizontal coordinates of all points, and y is an array of vertical coordinates of all points. In this paper, when drawing the cuff curve, four auxiliary points are used to determine the shape; when drawing

the back and front collar circumference curve, one auxiliary point is used to determine the shape separately.

5.4. Programming of PBP parametric pattern-making

In this study, a function program for PBP parametric pattern-making is written, named def PBP (C, B). The initial parameters in the function represent the chest girth and back length dimensions, respectively. When this program is running, the def PBP is called directly in the Command Window. The values of the initial parameters are entered to obtain the corresponding PBP directly.

5.5. Shirt pattern generation

The PBP obtained in this study can be directly applied to generate different styles of shirt patterns, including slim, regular and loose. The principle is based on the prototyping method, where the structured lines are lengthened, shortened, expanded and contracted according to the PBP to generate the garment patterns for different styles, as shown in Figure 9. Although the pattern of men's shirts includes the front and back pieces, collar and sleeves (Cunnington and Cunningham

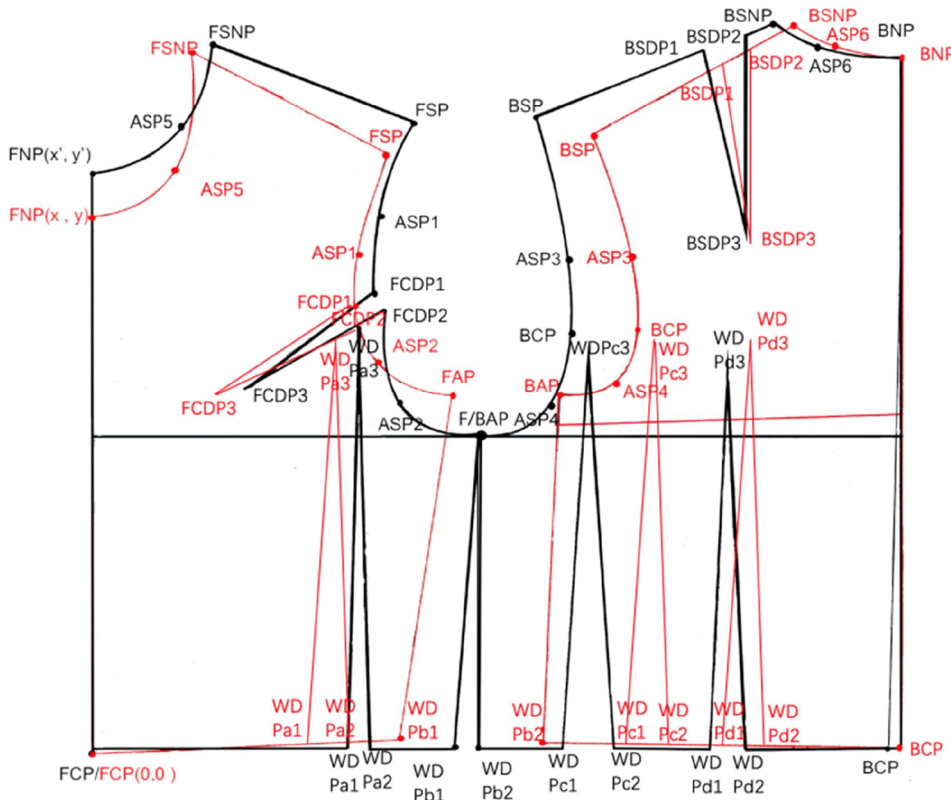


Figure 7. Correspondence points on the New Bunka basic pattern (Black) and PBP (Red).

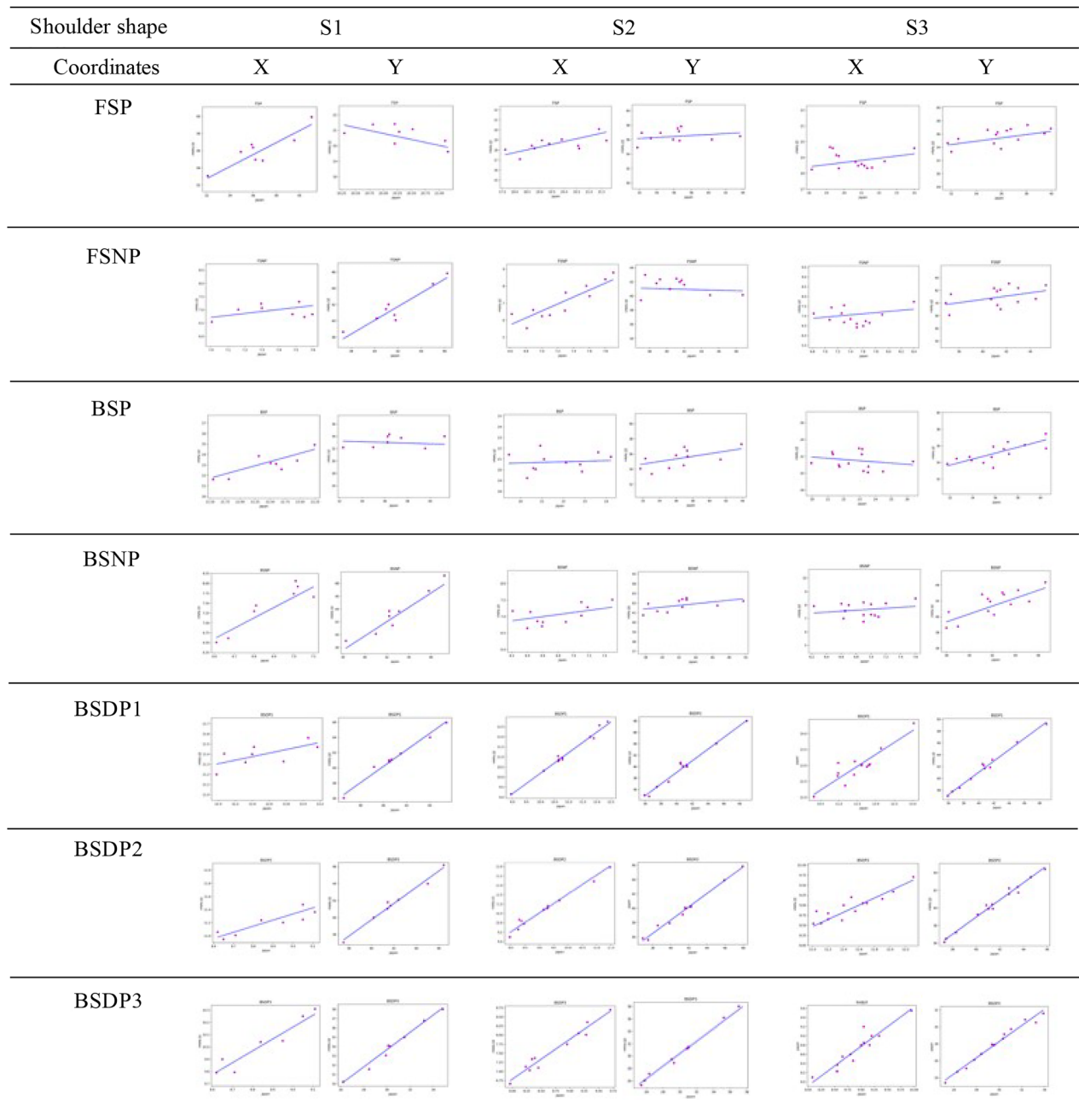


Figure 8. Key feature points linear regression models on shoulder.

1992; Brough 2008), this study focuses on improving the fit of the garment, so we mainly consider the generation of the front and back pieces of the garment. The generated shirt pattern is named PBP_{shirt}. The structured relationship between the PBP and the PBP_{shirt} is shown in Table 9.

The pattern structure analysis shows that differences of the shirt styles depend on two factors: the waist dart of the back piece and the dart of the side seam. After the parametric pattern is built, if the user is not satisfied with the style effect, the adjustable input (dart ease

allowance) and appearance parameter (garment length) can be modified to quickly produce a personalised shirt pattern. The expressions can be given a definite value for each user's specific dimension and requirement so that one person can have one garment pattern.

In this study, a function program for PBP_{shirt} parametric pattern-making is written, named def PBP_{shirt}. When this program is running, both the def PBP and def PBP_{shirt} are called directly in the Command Window. The values of the initial parameters are entered to obtain the corresponding PBP_{shirt} directly.

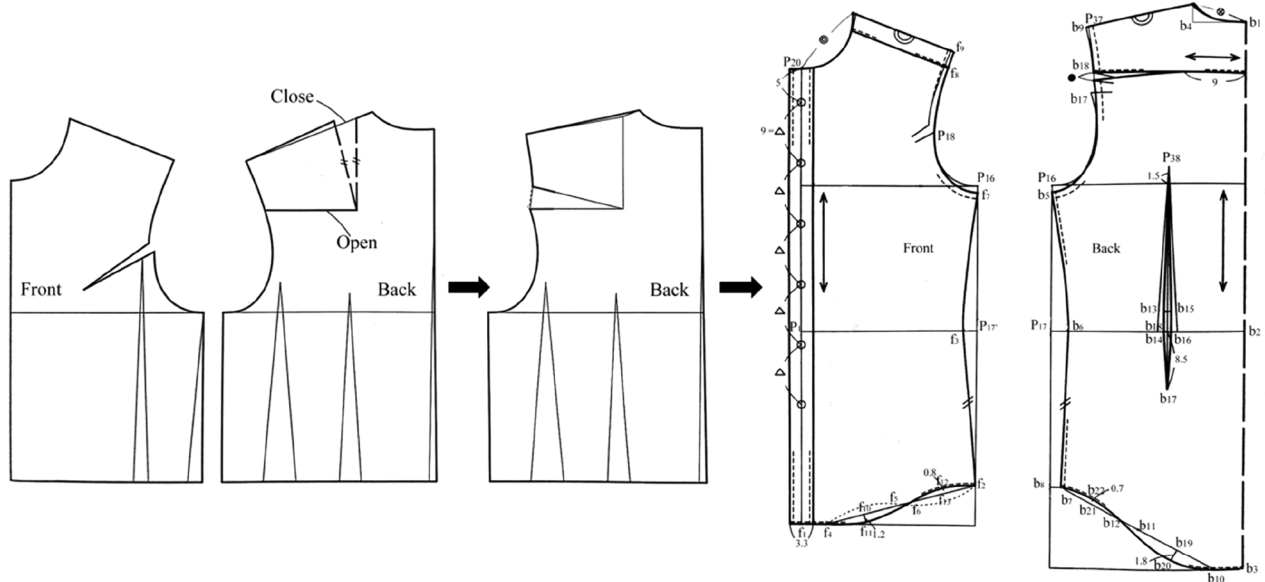


Figure 9. Men's shirt body pattern making method based on PBP pattern.

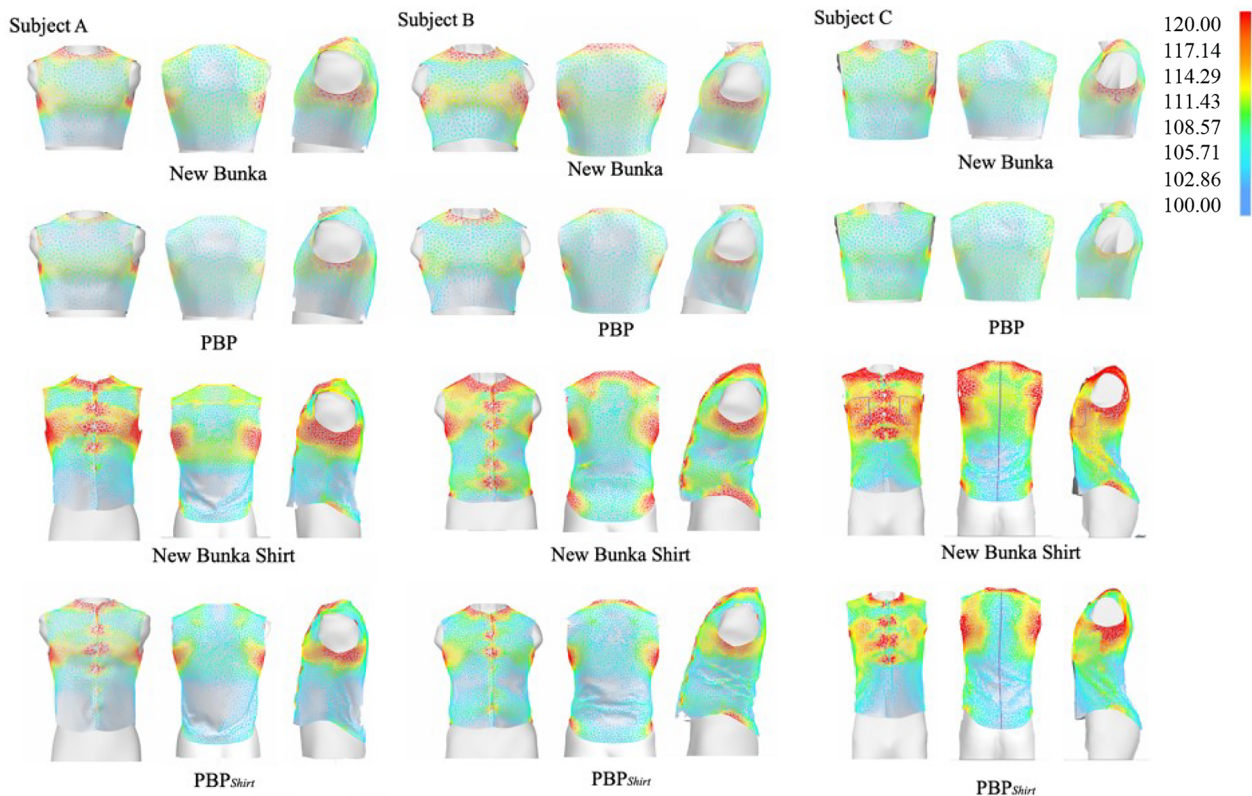


Figure 10. Virtual try-on strain map for slim style shirt.

5.6. Visual evaluation

After the parametric garment pattern is generated, it must be verified whether it can be applied to the apparel industry. The PBP and PBP_{Shirt} are fitted separately to correspond corrected human body models

(such as Figure 8(g) but without the mesh) by using the 2D-to-3D virtual try-on method (Liu et al., 2016; Tao et al. 2018). Furthermore, the strain map generated by the 3D garment is visually evaluated.

Table 9. Rules for changing from PBP to men's shirt bodices.

Garment pattern	Line	Rule changes	Garment pattern	Line	Rule changes
Back	b1b2	B+0,5	Front	f1P1	29
	b2b3	35		f1f4	2
	b1b4	N/5-0,5		f5f6	1.5
	b5P16	1	f4f5, f2f5	1/2* f2f4	
	b6P17	2.5		f4f10	1/2* f5f4
	b8P17	23		f6f13	1/2* f6f2
	b7b8	1.5		f10f11	1.2
	b3b10	4		f12f13	0.8
	b10b11	1/2* b7b10		f7P16	1
	b11b12	3		f3P17'	2
	b13b14,	5		f8f9	2.5
	b15b16				
	b13b15,	1			
	b14b16				
	b17 b18	8.5			
	b11b19	1/2* b11b10			
	b20b19	1.8			
	b21b7	1/2* b7b12			
	b21b22	0.7			
	*	2/5* b17b18			

Note: *N* stands for neck girth and *B* stands for back length. All units are in cm.

6. Result and discussion

So far, we have mainly introduced a regression model to obtain PBP by adjusting the basic pattern and parametric modelling methods for the shirt pattern. To prove the feasibility of these methods, in this section, we evaluate the PBP and PBPshirt obtained through these two models separately, in terms of qualitative and quantitative results, and then provide further discussion.

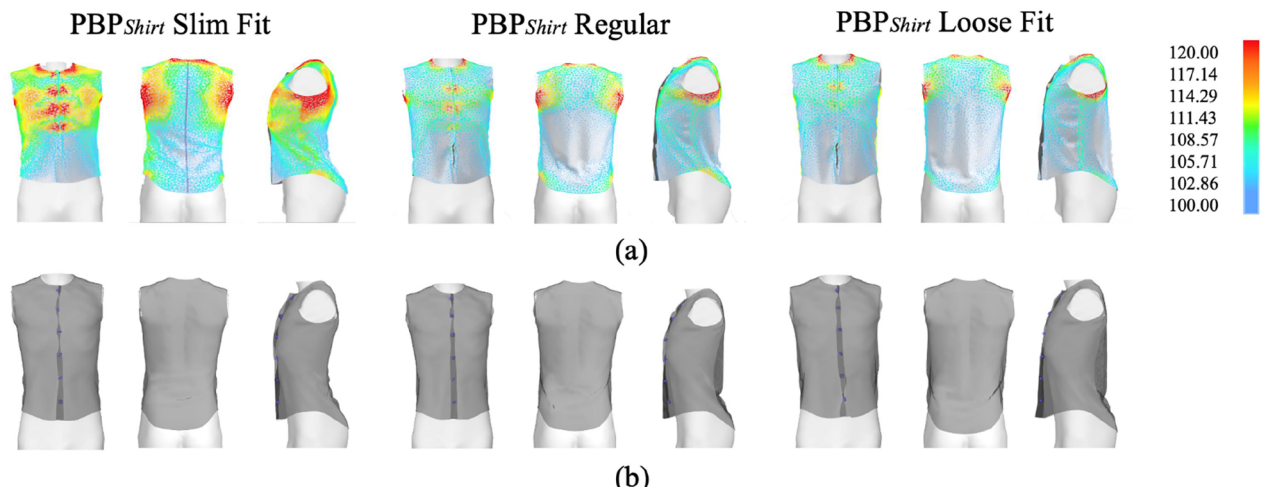
6.1. PBP's parametric pattern-making effect

To test the effect and practical value of the parametric pattern-making method proposed in the application in this paper, the chest girth and back length of three people with large differences in body shapes were measured and recorded as an example. Among them,

Table 10. Comparison of the strain map.

Subject	Garment pattern	Strain map distribution ratio			
		Red	Orang-Yellow	Green	Light-Dark Blue
A	New Bunka basic pattern	8.9%	15.8%	19.6%	55.6%
	PBP	3.8%	6.5%	46.8%	42.5%
B	New Bunka shirt pattern	17.4%	26.4%	14.9%	41.3%
	PBP _{shirt}	9.8%	15.7%	38.9%	35.4%
C	New Bunka basic pattern	12.7%	22.0%	17.5%	47.6%
	PBP	5.4%	9.1%	44.7%	40.3%
	New Bunka shirt pattern	19.7%	25.4%	13.3%	41.6%
	PBP _{shirt}	7.2%	11.3%	46.1%	35.2%
All Subjects Average	New Bunka basic pattern	4.6%	8.1%	26.7%	60.4%
	PBP	0.0%	5.7%	66.7%	27.6%
	New Bunka shirt pattern	22.1%	31.2%	19.7%	26.9%
	PBP _{shirt}	9.3%	20.0%	39.2%	32.1%
	New Bunka basic pattern	9.2%	14.8%	22.4%	53.5%
	PBP	3.6%	6.7%	51.7%	37.7%
	New Bunka shirt pattern	19.1%	29.4%	15.1%	36.3%
	PBP _{shirt}	8.8%	19.1%	41.9%	30.1%

Subject C

**Figure 11.** Virtual try-on for three styles of shirts: (a) strain map; (b) draping simulation.

Subject B (plump body shape) and Subject C (slim body shape) are new samples (not included in the previous 33 samples). Then, these dimensions are input into Python, and the functions written previously are called. The final generated PBPs are shown in Figure 10. Figure 10 shows a comparison of the strain maps of the virtual try-on (Yan and Kuzmichev 2020; Hidellaarachchi et al. 2018) effect of the PBP and New Bunka basic pattern. The strain map shows the degree of deformation that occurred after the garment was worn on the virtual model. The area of the colour zone represents the garment fit level. If the area shown is red, this indicates that the garment strains the body more than the body can handle. The orange to yellow area indicates that although the garment feels tight to the body when worn, it is tolerable. The green area indicates that the body does not put pressure on the garment, and the person wearing the garment feels comfortable and unrestrained. The light to dark blue area indicates that there is more space between the garment and the body. Therefore, the fit of the garment is not proper even though there is no tightness.

By comparison, it can be observed in Figure 10 that the PBP significantly improves the fit of the New Bunka basic pattern. The shoulder fit of subject A is significantly improved in PBP. Subject B's shoulder, arm root and chest fit are significantly improved in PBP. The shoulder and arm root fit of subject C is significantly improved in PBP. As is shown in Table 10, in the same way, the distribution ratio of the New Bunka basic pattern and PBP of 33 previous subjects are measured. The red areas on the strain maps of the 33 subjects decrease by an average of 5.6%, the orange to yellow areas decrease by an average of 8.7%, the light to dark blue areas decrease by an average of 15.8%, and the green areas increase by an average of 29.3%. This shows that the PBP has a better fit than the New Bunka basic pattern.

6.2. PBPshirt parametric pattern-making effect

The PBPshirt proposed in this paper are obtained by using the prototype making method based on the PBP. To test the effectiveness of this method in the application, PBPshirt is made based on the PBP that are obtained in the previous section. Taking the slim fit style as an example, the finally generated PBPshirt are shown in Figure 10. By comparing the strain maps of the virtual try-on effect of the PBPshirt and the New Bunka shirt version (Fengqin et al. 2017), it can be seen that the PBPshirt fit better than the New Bunka shirt pattern. As is shown in Table 10, compared to the New Bunka shirt pattern, the red areas on the

strain maps of the 33 previous subjects decrease by an average of 10.3%, the orange to yellow areas decrease by an average of 10.3%, the light to dark blue areas decrease by an average of 6.2% and the green areas increase by an average of 26.8%. This shows that the PBPshirt has a better fit than the New Bunka shirt pattern. Although there is an increase in the light to dark blue areas of subjects like subject C, the increments are not large. Based on the virtual try-on view and designer's experience, this level of increment is not enough to cause the shirt to be excessively loose and thus can be accepted.

6.3. PBPshirt in different styles

The main consideration of this study is fit-oriented parametric garment pattern design. Therefore, three styles (slim, regular and loose) of shirt patterns were validated in CLO 3D using the same fabric that comes with the software. As an example, the results of subject C are shown in Figure 11. The evaluation is performed by professional garment pattern makers and designers.

When making the parametric pattern for the three styles of shirt, only the waist darts volumes were adjusted, and the other parameters remained the same. As can be seen from the try-on strain maps for all three styles (Figure 11(a)), all shirts show an overall good garment fit. As can be seen in the semi-transparent draping simulation for all three styles (Figure 11(b)), from the slim fit style to the loose fit style, the amount of folds due to stress (not fit) decreases and the amount of natural draping folds increases. The volume of the garment body becomes larger. At the same time, the position and dimension of the neckline, shoulder line and sleeve holes remain the same. According to the observation result from experts, the PBPshirt parametric pattern-making method can be applied to different shirt styles, from slim to lose, with assured high-level garment fit.

In addition, using parametric pattern making, designers can easily handle complex curves in a garment pattern and do not need to calculate the relationship of the structure and position of complex curves because the program can automatically draw complex curves according to the internal structure of the garment and the value of the parameters, which significantly improves the efficiency and accuracy of the pattern design.

7. Conclusion

In the current apparel industry, the existing parametric garment pattern-making models have only considered the differences in human body dimensions. They lack

consideration of body shape differences. Therefore, users cannot find suitable clothes often. In this situation, this paper proposes a personalised garment pattern recommendation system which is oriented to fit by integrating the designer's knowledge and 3D measurement. The final generated garment pattern considers the influence of body dimension and body part shape and the user's requirement of style. The proposed recommendation system can rapidly, accurately and automatically generate PBPshirt by a linear regression model (from basic pattern to PBP) and parametric model based on the prototype making method (from PBP to PBPshirt). From a comprehensive quantitative analysis, we find that the average of the PBP fit areas has been improved by 29.3% compared with the New Bunka basic pattern. The average of the PBPshirt fit areas has been increased by 26.8% compared with the New Bunka shirt pattern. Meanwhile, the average of PBP and PBPshirt unfit areas (red areas, orange to yellow areas, light to dark blue areas) have been decreased in different degrees. In addition, our proposed method saves plenty of time for designers, and the cost of the shirt's development reduces distinctly. Even users with no pattern-making knowledge can also develop professional shirt patterns by using our proposed system.

In the future work, the feasibility of the parametric garment pattern-making model in the apparel industry will be further explored by developing different garment pattern design processes. Also, the proposed modelling procedure will be extended from the men's top garment to their lower garment and female garment.

Disclosure statement

No potential conflict of interest was reported by the author(s).

Ethical

There is no Ethical statement was reported by the author(s).

Funding

There is no Funding to report for this submission.

References

- Belhadi, Amine, Karim Zkik, Anass Cherrafi, Sha'ri M. Yusof, and Said El Fezazi. 2019. "Understanding Big Data Analytics for Manufacturing Processes: insights from Literature Review and Multiple Case Studies." *Computers & Industrial Engineering* 137: 106099. doi:[10.1016/j.cie.2019.106099](https://doi.org/10.1016/j.cie.2019.106099).
- Brough, D M G. 2008. *Neo-Dandy: wearability, Design Innovation and the Formal White Dress Shirt for Men* (Doctoral dissertation, Queensland University of Technology).
- Chan, A. P., J. Fan, and W. Yu. 2003. "Men's Shirt Pattern Design Part II: Prediction of Pattern Parameters from 3D Body Measurements." *Sen'i Gakkaishi* 59 (8): 328–333. doi:[10.2115/fiber.59.328](https://doi.org/10.2115/fiber.59.328).
- Chi, Cheng, Xianyi Zeng, Pascal Bruniaux, and Guillaume Tartare. 2022. "A Study on Segmentation and Refinement of Key Human Body Parts by Integrating Manual Measurements." *Ergonomics* 65 (1): 60–77. doi:[10.1080/00140139.2021.1963489](https://doi.org/10.1080/00140139.2021.1963489).
- Chi, Cheng, Xianyi Zeng, Pascal Bruniaux, Guillaume Tartare, and Hongshu Jin. 2022. "A New Parametric 3D Human Body Modeling Approach by Using Key Position Labeling and Body Parts Segmentation." *Textile Research Journal* 92 (19-20): 3653–3679. doi:[10.1177/00405175221089688](https://doi.org/10.1177/00405175221089688).
- Cui, L. 2016. *The Establishment of Blouse'S Parameter Constraint Database Based on Pattern Automatic Generation[C]//2016 2nd International Conference on Advances in Energy, Environment and Chemical Engineering (AEECE 2016)* (pp. 1–4). Atlantis Press. doi:[10.2991/aeece-16.2016.1](https://doi.org/10.2991/aeece-16.2016.1).
- Cunnington, C W., and P. Cunnington. 1992. *The History of Underclothes*. Courier Corporation.
- Deivanayagam, S. 1992. "Designing for Maintainability: computerized Human Models." *Computers & Industrial Engineering* 23 (1-4): 195–196. doi:[10.1016/0360-8352\(92\)90096-3](https://doi.org/10.1016/0360-8352(92)90096-3).
- Dianat, I., J. Molenbroek, and H I. Castellucci. 2018. "A Review of the Methodology and Applications of Anthropometry in Ergonomics and Product Design." *Ergonomics* 61 (12): 1696–1720. doi:[10.1080/00140139.2018.1502817](https://doi.org/10.1080/00140139.2018.1502817).
- Dziuban, C D., and E C. Shirkey. 1974. "When is a Correlation Matrix Appropriate for Factor Analysis? Some Decision Rules." *Psychological Bulletin* 81 (6): 358–361. doi:[10.1037/h0036316](https://doi.org/10.1037/h0036316).
- Fan, Hao, Suihuai Yu, Jianjie Chu, Mengcheng Wang, Dengkai Chen, Shuai Zhang, Wenzhong Wang, Tong Wu, and Ning Wang. 2019. "Anthropometric Characteristics and Product Categorization of Chinese Auricles for Ergonomic Design." *International Journal of Industrial Ergonomics* 69: 118–141. doi:[10.1016/j.ergon.2018.11.002](https://doi.org/10.1016/j.ergon.2018.11.002).
- Fengqin, XIA., WU. Ge, XIE. Haoyang, and ZHONG. Yueqi. 2017. "Classification of Body Shape Based on Longitudinal Section Curve XIA." *Journal of Textile Research* 38 (06): 86–91.
- Greder, K C., J. Pei, and J. Shin. 2020. "Design in 3D: A Computational Fashion Design Protocol." *International Journal of Clothing Science and Technology* 32 (4): 537–549. doi:[10.1108/IJ CST-07-2019-0110](https://doi.org/10.1108/IJ CST-07-2019-0110).
- Gu, B., and G. Liu. 2013. "Research on Structural Design of Pants and Pattern Generation System." *Journal of Multimedia* 8 (6) doi:[10.4304/jmm.8.6.809-815](https://doi.org/10.4304/jmm.8.6.809-815).
- Gu, B., G. Liu, and B. Xu. 2017. "Individualizing Women's Suit Patterns Using Body Measurements from Two-Dimensional Images." *Textile Research Journal* 87 (6): 669–681. doi:[10.1177/0040517516636001](https://doi.org/10.1177/0040517516636001).
- Gu, Y., and Y. Shi. 2019. "Research on Automatic Method of Curves Drawing in Garment CAD Pattern System." *Computer Science and Application* 9 (1): 9–18.
- Hamad, M., S. Thomassey, and P. Bruniaux. 2017. "A New Sizing System Based on 3D Shape Descriptor for Morphology Clustering." *Computers & Industrial Engineering* 113: 683–692. doi:[10.1016/j.cie.2017.05.030](https://doi.org/10.1016/j.cie.2017.05.030).
- Hammond, Peter, Tim J. Hutton, Judith E. Allanson, Linda E. Campbell, Raoul C M. Hennekam, Sean Holden, Michael A. Patton, Adam Shaw, I Karen Temple, Matthew Trotter,

- Kieran C. Murphy, and Robin M. Winter. 2004. "3D Analysis of Facial Morphology." *American Journal of Medical Genetics. Part A* 126A (4): 339–348. doi:[10.1002/ajmg.a.20665](https://doi.org/10.1002/ajmg.a.20665).
- He, C J., B A. Ying, X F. Wang., et al. 2021. "Construction and Application of Clothing Pattern Design Model Based on Directed Graph Method." *Journal of Fiber Bioengineering and Informatics* 14 (1): 41–51. doi:[10.3993/jfbim00347](https://doi.org/10.3993/jfbim00347).
- Hidellaarachchi, D., H. Gunatilake, S. Perera., et al. 2018. *Towards a Virtual Garment Fitting Model for Male Upper Body for Online Marketplace/2018 18th International Conference on Advances in ICT for Emerging Regions (ICTer)* (pp. 322–331). IEEE.
- Hinds, B K., J. McCartney, and G. Woods. 1991. "Pattern Development for 3D Surfaces." *Computer-Aided Design* 23 (8): 583–592. doi:[10.1016/0010-4485\(91\)90060-A](https://doi.org/10.1016/0010-4485(91)90060-A).
- Hong, Y., P. Bruniaux, and J. Zhang. 2018. "Application of 3D-to-2D Garment Design for Atypical Morphology: A Design Case for Physically Disabled People with Scoliosis." *Industria Textila* 69 (1): 59–64.
- Hong, Yan., Xianyi Zeng, Pascal Bruniaux, and Kaixuan Liu. 2016. "Interactive Virtual Try-on Based Three-Dimensional Garment Block Design for Disabled People of Scoliosis Type." *Textile Research Journal*. 87 (10): 1261–1274. doi:[10.1177/0040517516651105](https://doi.org/10.1177/0040517516651105).
- Huang, C Y. 2014. "Study on Classification of Body Shape and Size Grading on Young Women of Quanzhou District/ Advanced Materials Research." *Advanced Materials Research* 989-994: 5319–5322. doi:[10.4028/www.scientific.net/AMR.989-994.5319](https://doi.org/10.4028/www.scientific.net/AMR.989-994.5319).
- Huang, Xizhang, Gang Wang, Chao Chen, Jiangshan Liu, Bjorn Kristiansen, Andreas Hohmann, and Kewei Zhao. 2021. "Constructing a Talent Identification Index System and Evaluation Model for Cross-Country Skiers." *Journal of Sports Sciences* 39 (4): 368–379. doi:[10.1080/02640414.2020.1823084](https://doi.org/10.1080/02640414.2020.1823084).
- Jeang, Angus, An Jen Chiang, Po Cheng Chiang, Po Sheng Chiang, and Pei Yu Tung. 2018. "Robust Parameters Determination for Ergonomical Product Design via Computer Musculoskeletal Modeling and Multi-Objective Optimization." *Computers & Industrial Engineering* 118: 180–201. doi:[10.1016/j.cie.2018.02.013](https://doi.org/10.1016/j.cie.2018.02.013).
- Jin, S.-N., B.-F. Gu, B.-B. Zhang, Y.-P. Xia, and H.-Z. He. 2023. "Pants Design and Pattern Generation Based on Body Images." *Industria Textila* 74 (01): 74–80. doi:[10.35530/IT.074.01.20223](https://doi.org/10.35530/IT.074.01.20223).
- Kang, T J., and S M. Kim. 2000. "Optimized Garment Pattern Generation Based on Three-Dimensional Anthropometric Measurement." *International Journal of Clothing Science and Technology* 12(4), 240–254.
- Kim, KyoungOk, Noriaki Innami, Masayuki Takatera, Tadaharu Narita, Midori Kanazawa, and Yuji Kitazawa. 2017. "Individualized Male Dress Shirt Adjustments Using a Novel Method for Measuring Shoulder Shape." *International Journal of Clothing Science and Technology* 29 (2): 215–225. doi:[10.1108/IJ CST-02-2016-0011](https://doi.org/10.1108/IJ CST-02-2016-0011).
- Kim, S., and C K. Park. 2007. "Basic Garment Pattern Generation Using Geometric Modeling Method." *International Journal of Clothing Science and Technology* 19 (1): 7–17. doi:[10.1108/09556220710717017](https://doi.org/10.1108/09556220710717017).
- Lei, J., X. You, and M. Abdel-Mottaleb. 2016. "Automatic Ear Landmark Localization, Segmentation, and Pose Classification in Range Images." *IEEE Transactions on Systems, Man, and Cybernetics: Systems* 46 (2): 165–176. doi:[10.1109/TSMC.2015.2452892](https://doi.org/10.1109/TSMC.2015.2452892).
- Leong, I F., J J. Fang, and M J. Tsai. 2007. "Automatic Body Feature Extraction from a Marker-Less Scanned Human Body." *Computer-Aided Design* 39 (7): 568–582. doi:[10.1016/j.cad.2007.03.003](https://doi.org/10.1016/j.cad.2007.03.003).
- Liu, Haisang, Gaoming Jiang, Zhijia Dong, Fenglin Xia, and Honglian Cong. 2020. "The Size Prediction and Auto-Generation of Garment Template." *International Journal of Clothing Science and Technology* 33 (1): 74–92. doi:[10.1108/IJ CST-06-2019-0083](https://doi.org/10.1108/IJ CST-06-2019-0083).
- Liu, K., J. Wang, and Y. Hong. 2017. "Wearing Comfort Analysis from Aspect of Numerical Garment Pressure Using 3D Virtual-Reality and Data Mining Technology." *International Journal of Clothing Science and Technology* 29 (2): 166–179. doi:[10.1108/IJ CST-03-2016-0017](https://doi.org/10.1108/IJ CST-03-2016-0017).
- Liu, Kaixuan, Jianping Wang, Edwin Kamalha, Victoria Li, and Xianyi Zeng. 2017. "Construction of a Prediction Model for Body Dimensions Used in Garment Pattern Making Based on Anthropometric Data Learning." *The Journal of the Textile Institute* 108 (12): 2107–2114. doi:[10.1080/004050000.2017.1315794](https://doi.org/10.1080/004050000.2017.1315794).
- Liu, Kaixuan, Jianping Wang, Chun Zhu, and Yan Hong. 2016. "Development of Upper Cycling Clothes Using 3D-to-2D Flattening Technology and Evaluation of Dynamic Wear Comfort from the Aspect of Clothing Pressure." *International Journal of Clothing Science and Technology* 28 (6): 736–749. doi:[10.1108/IJ CST-02-2016-0016](https://doi.org/10.1108/IJ CST-02-2016-0016).
- Liu, Kaixuan, Xianyi Zeng, Pascal Bruniaux, Xuyuan Tao, Xiaofeng Yao, Victoria Li, and Jianping Wang. 2018. "3D Interactive Garment Pattern-Making Technology." *Computer-Aided Design* 104: 113–124. doi:[10.1016/j.cad.2018.07.003](https://doi.org/10.1016/j.cad.2018.07.003).
- Liu, Kaixuan, Xianyi Zeng, Pascal Bruniaux, Jianping Wang, Edwin Kamalha, and Xuyuan Tao. 2017. "Fit Evaluation of Virtual Garment Try-on by Learning from Digital Pressure Data." *Knowledge-Based Systems* 133: 174–182. doi:[10.1016/j.knosys.2017.07.007](https://doi.org/10.1016/j.knosys.2017.07.007).
- Liu, Kaixuan, Xianyi Zeng, Jianping Wang, Xuyuan Tao, Jun Xu, Xiaowen Jiang, Jun Ren, Edwin Kamalha, Tarun-Kumar Agrawal, and Pascal Bruniaux. 2018. "Parametric Design of Garment Flat Based on Body Dimension." *International Journal of Industrial Ergonomics* 65: 46–59. doi:[10.1016/j.ergon.2018.01.013](https://doi.org/10.1016/j.ergon.2018.01.013).
- Malhotra, Deepika, Sharadwata Pan, Lars Rüther, Thomas B. Goudoulas, Gerrit Schlippe, Werner Voss, and Natalie Germann. 2019. "Linear Viscoelastic and Microstructural Properties of Native Male Human Skin and in Vitro 3D Reconstructed Skin Models." *Journal of the Mechanical Behavior of Biomedical Materials* 90: 644–654. doi:[10.1016/j.jmbbm.2018.11.013](https://doi.org/10.1016/j.jmbbm.2018.11.013).
- Malti, A. 2021. "On the Exact Recovery Conditions of 3D Human Motion from 2D Landmark Motion with Sparse Articulated Motion." *Computer Vision and Image Understanding* 202: 103072. doi:[10.1016/j.cviu.2020.103072](https://doi.org/10.1016/j.cviu.2020.103072).
- Mashiko, MIYOSHI. 2006. *Clothing Modelling Learning: Theory[M]*. ZHENG Rong. Translating. Beijing: China Textile&Apparel Press,
- Peres, S C., R K. Mehta, and P. Ritchey. 2017. "Assessing Ergonomic Risks of Software: Development of the SEAT." *Applied Ergonomics* 59 (Pt A): 377–386. doi:[10.1016/j.apergo.2016.09.014](https://doi.org/10.1016/j.apergo.2016.09.014).
- Pierola, A., I. Epifanio, and S. Alemany. 2016. "An Ensemble of Ordered Logistic Regression and Random Forest for Child Garment Size Matching." *Computers & Industrial Engineering* 101: 455–465. doi:[10.1016/j.cie.2016.10.013](https://doi.org/10.1016/j.cie.2016.10.013).

- Song, H K., and S P. Ashdown. 2012. "Development of Automated Custom-Made Pants Driven by Body Shape." *Clothing and Textiles Research Journal* 30 (4): 315–329. doi: [10.1177/0887302X12462058](https://doi.org/10.1177/0887302X12462058).
- Su, J., Y. Ke, B. Gu., et al. 2017. "A Method to Develop a Personalized Pattern of Pant from 3D Scanning Data." *Proceedings of 3dbody. tech 2017– 8th International Conference and Exhibition on 3D Body Scanning and Processing Technologies, Montreal, Canada, 11–12 October 2017*, pp. 121–129.
- Su, J., G. Liu, and B. Xu. 2015. "Development of Individualized Pattern Prototype Based on Classification of Body Features." *International Journal of Clothing Science and Technology* 27 (6): 895–907. doi: [10.1108/IJCST-11-2014-0136](https://doi.org/10.1108/IJCST-11-2014-0136).
- Tao, Xuyuan, Xiao Chen, Xianyi Zeng, and Ludovic Koehl. 2018. "A Customized Garment Collaborative Design Process by Using Virtual Reality and Sensory Evaluation on Garment Fit." *Computers & Industrial Engineering* 115: 683–695. doi: [10.1016/j.cie.2017.10.023](https://doi.org/10.1016/j.cie.2017.10.023).
- Thomassey, S., and P. Briniaux. 2013. "A Template of Ease Allowance for Garments Based on a 3D Reverse Methodology." *International Journal of Industrial Ergonomics* 43 (5): 406–416. doi: [10.1016/j.ergon.2013.08.002](https://doi.org/10.1016/j.ergon.2013.08.002).
- Wang, Y. 2020. *Digitalization of Garment Design Based on CorelDRAW Software. Computer-Aided Design and Applications* 17 (S2): 111–122.
- Wang, Zhujun, Jianping Wang, Yingmei Xing, Yalan Yang, and Kaixuan Liu. 2019. "Estimating Human Body Dimensions Using RBF Artificial Neural Networks Technology and Its Application in Activewear Pattern Making." *Applied Sciences* 9 (6): 1140. doi: [10.3390/app9061140](https://doi.org/10.3390/app9061140).
- Wang, Weijie, Gaopeng Zhang, Luming Yang, and Wei Wang. 2019. "Research on Garment Pattern Design Based on Fractal Graphics." *EURASIP Journal on Image and Video Processing* 2019 (1): 1–15. doi: [10.1186/s13640-019-0431-x](https://doi.org/10.1186/s13640-019-0431-x).
- Xiu, Y., and Z K. Wan. 2013. "A Survey on Pattern-Making Technologies in Garment CAD. In *IEEE Conference Anthology* (pp. 1–6). IEEE.
- Yan, J., and V E. Kuzmichev. 2020. "A Virtual e-Bespoke Men's Shirt Based on New Body Measurements and Method of Pattern Drafting." *Textile Research Journal* 90 (19–20): 2223–2244. doi: [10.1177/0040517520913347](https://doi.org/10.1177/0040517520913347).
- Yong, A G., and S. Pearce. 2013. "A Beginner's Guide to Factor Analysis: Focusing on Exploratory Factor Analysis." *Tutorials in Quantitative Methods for Psychology* 9 (2): 79–94. doi: [10.20982/tqmp.09.2.p079](https://doi.org/10.20982/tqmp.09.2.p079).
- Yumiko, ITO., et al. 2006. *Bunka Fashion System Lecture (9) Fashion Design*, Bunka Publishing Bureau, 37–39.
- Zakaria, N. 2014. *Body Shape Analysis and Identification of Key Dimensions for Apparel Sizing Systems/Anthropometry, Apparel Sizing and Design* (pp. 95–119). Woodhead Publishing.
- Zhou, Q., L. He, and R. Li. 2017. "Research on the Application of Personalized Customized Virtual Design Method in Clothing." *DEStech Transactions on Computer Science and Engineering* 39–49. doi: [10.12783/dtcse/cii2017/17228](https://doi.org/10.12783/dtcse/cii2017/17228).